

Effect of intermolecular orientation upon proton transfer within a polarizable medium

Steve Scheiner and Xiaofeng Duan

Department of Chemistry and Biochemistry, Southern Illinois University, Carbondale, Illinois 62901

ABSTRACT *Ab initio* calculations are used to investigate the proton transfer process in bacteriorhodopsin. $\text{HN}=\text{CH}_2$ serves as a small prototype of the Schiff base while HCOO^- models its carboxylate-containing counterion and HO^- the hydroxyl group of water of tyrosine, leading to the $\text{HCOO}^- \cdots \text{H}^+ \cdots \text{NHCH}_2$ and $\text{HO}^- \cdots \text{H}^+ \cdots \text{NHCH}_2$ complexes. In isolation, both complexes prefer a neutral pair configuration wherein the central proton is associated with the anion. However, the Schiff base may be protonated in the former complex, producing the $\text{HCOO}^- \cdots \text{H}^+ \text{NHCH}_2$ ion pair, when there is a high degree of dielectric coupling with an external polarizable medium. Within a range of intermediate level coupling, the equilibrium position of the proton (on either the carboxylate or Schiff base) can be switched by suitable changes in the intermolecular angle. pK shifts resulting from a 60° reorientation are calculated to be some 5–12 pK U within the coupling range where proton transfers are possible. The energy barrier to proton transfer reinforces the ability of changes in angle and dielectric coupling to induce a proton transfer.

INTRODUCTION

The question of whether a proton is associated with one group of a hydrogen-bonding pair or its partner is of great importance in the mechanism of a number of proteins (1–3). The shuttling of a proton from serine to histidine must occur in serine proteinases in order for the former residue to attack the peptide substrate (4). In an example central to bioenergetics, it is the proton release from the Schiff base of the bacteriorhodopsin chromophore, resulting from earlier photon absorption, that enables the protein to pump protons against the chemical gradient of the biomembrane (5–7). The mechanism whereby protons are held on one group of a protein until the appropriate point in the reaction, and then released to another group remains poorly understood.

One way of attacking the unanswered questions of proton transfer on a fundamental level is via *ab initio* quantum mechanical calculations. Sets of calculations have been carried out in this laboratory and others over the years (8–13) to seek an understanding of the proton transfer process in an isolated setting, free of external influences. A number of interesting principles have emerged which may have direct bearing on the problem, even in the context of a protein molecule. For example, the barrier to proton transfer is surprisingly sensitive to the distance separating the two groups involved in the transfer (8, 14–16). Hence, transfers across long H-bonds become untenable for time scales appropriate to enzymatic activity (17). It appears also that the equilibrium position of a proton can be shifted from one group to its partner by certain adjustments of the angular character-

istics of the H bond that connects them (18–21). Principles such as these could have obviously far reaching implications in how proteins are able to control proton states of various residues.

Before these principles can be applied, however, it is first essential to determine how the influence of a protein-like environment modulates the set of rules developed for *in vacuo* transfers. Past work in this laboratory has addressed the issue of neighboring ions and permanent dipoles (22, 23). It has been found that these entities exert their influence on the proton transfer through electrostatic force which is a purely additive phenomenon. Interestingly, the H-bond appears to magnify this force relative to what would be expected for a naked proton. In addition to particular polar species, the protein environment consists of a large number of polarizable groups extending throughout the entire macromolecule. The purpose of this communication is to examine the latter effect in some detail.

In particular, we focus on the Schiff base because of its known importance in bacteriorhodopsin. Although the precise nature of its counterion remains uncertain, recent evidence indicates it to be the carboxylate group of Asp (6, 24–29). We therefore concentrate our efforts on the protonated Schiff base–Asp pair, modeled here by H_2CNH_2^+ and HCOO^- . We ask the question as to whether angular readjustments of the H-bond connecting them can induce a proton transfer within the protein environment or in an *in vacuo* situation. The problem is studied over a range of strength of the coupling with the polarizable environment. Also investigated is the dis-

tance dependence of the transfer barrier: how does interaction with a dielectric medium affect this behavior? As a point of comparison with HCOO^- , we also consider the stronger base OH^- which can occur itself or serve as a model of the hydroxyl group of Ser or Tyr.

METHODS

Ab initio calculations were carried out using the 4-31G basis set (30). The Gaussian 86 and 88 codes (31) were used for geometry optimizations and for in vacuo calculations. The self consistent reaction field approach, as implemented in the MONSTERGAUSS program (32), was used to place the system within a spherical cavity carved out of a dielectric continuum.

The deprotonation energies of CH_2NH_2^+ , HCOOH , and HOH were computed as the difference in energy between each species and the respective deprotonated moiety, viz, CH_2NH and the anions HCOO^- and OH^- , allowing full geometry optimization of each. These proton affinities are reported in Table 1 where they are compared with experimental data. The entries in the first column refer to the purely electronic contributions, i.e., the difference in electronic energy between AH^+ on one hand and $\text{A} + \text{H}^+$ on the other (the electronic energy of the proton is zero). ΔH is obtained after adding in nuclear contributions, viz, vibrational zero-point energies, translational, and rotational effects, as well as a ΔnRT term.

Not unexpectedly, there are discrepancies between the SCF/4-31G and experimental deprotonation energies, due to the fairly small size of the basis set and lack of correlation. These discrepancies amount to some 7 kcal/mol for H_2CNH_2^+ and HCOOH , and ~27 kcal/mol for HOH . However, what is most important for our purposes is not the deprotonation energy per se, but rather the difference from one molecule to the next. For example, the best available information indicates that it requires 131 kcal/mol more energy to remove a proton from HCOOH than from H_2CNH_2^+ (33, 35). This result is precisely reproduced at the SCF/4-31G level. The situation is not quite as favorable for the $\text{HOH}/\text{H}_2\text{CNH}_2^+$ pair where the latter is more acidic by some 177 kcal/mol, somewhat smaller than the SCF/4-31G difference of 194. It may be concluded that the level of theory used here will treat extremely well the competition for the proton between HCOO^- and H_2CNH , but the HO^- anion will have a slightly inflated preference in comparison to H_2CNH .

Tapia's formulation of the self consistent reaction field (SCRf) approach (36–39) was used to incorporate the effects of an external dielectric medium. The system of interest is placed within a spherical cavity of radius a hollowed out of a medium, characterized by

TABLE 1 Deprotonation energies

	ΔE_{elec}	$\Delta\text{H}(300\text{ K})^*$	$\Delta\text{H}_{\text{expt}}$
		<i>kcal/mol</i>	
CH_2NH_2^+	230.3 [‡]	221.9	214.3 [‡]
HCOOH	360.0 [§]	352.6	345.2 [‡]
HOH	426.0 [§]	418.3	391.3 [‡]

*Obtained by adding zero-point vibrational terms, translational, and rotational corrections and ΔnRT to electronic contribution.

[‡]From reference 33.

[§]MP3/6-31G** calculated value with appropriate corrections from reference 33.

[¶]From reference 34.

[†]From reference 35. *elec*, electronic; *expt*, experimental.

dielectric constant ϵ . Within the framework of the classical Kirkwood–Onsager theory, the coupling between the system and the medium is characterized by a reaction field susceptibility

$$g = (2/a^3) [(\epsilon - 1)/(2\epsilon + 1)]. \quad (1)$$

After multiplication by the square of the dipole moment operator, $g\mu^2$ is added to the Hamiltonian to account for the electrical polarization of the medium. Below, g will be expressed in units of \AA^{-3} , consistent with Eq. 1.

IN VACUO RESULTS

Several different conformations were examined for the complex pairing CH_2NH_2^+ with HCOO^- . As illustrated in Fig. 1, in all cases, the O—H group of HCOOH was allowed to form a hydrogen bond with the nitrogen atom of CH_2NH . The syn and anti-geometries of the complex refer to the corresponding arrangement of HCOOH wherein the OH proton is respectively *cis* or *trans* to the other oxygen atom. The syn-C structure is similar to syn

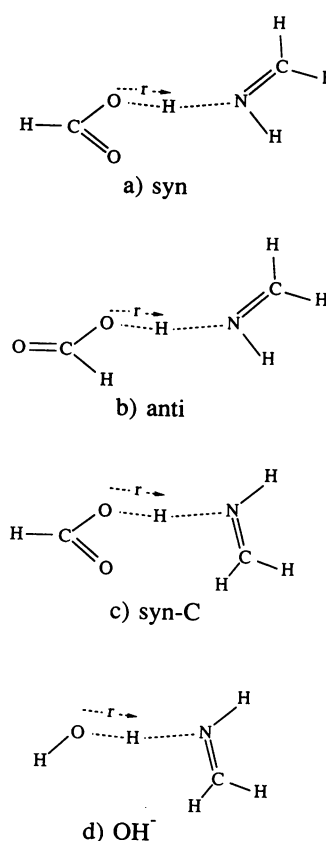


FIGURE 1 Disposition of atoms in various geometric arrangements of $\text{HCOO}^- \cdots \text{H}^+ \cdots \text{NHCH}_2$ and $\text{HO}^- \cdots \text{H}^+ \cdots \text{NHCH}_2$. R refers to distance between H-bonding O and N atoms. α is the C—O \cdots N angle for the former system and the C=N \cdots O angle for the latter.

above except that it is the CH₂ of CH₂NH that is proximate to the carbonyl oxygen rather than the H atom.

In each case, a proton transfer potential was traced out for a given intermolecular $R(\text{O}\cdots\text{N})$ distance. A series of different $r(\text{OH})$ distances r was chosen and for each, the geometry of the entire complex was fully optimized, subject only to the restriction of fixed R and r . For distances of $R = 2.75$ and 3.0 Å, the potentials contain two wells, as illustrated in Fig. 2. The leftmost well wherein r equals 0.95 Å or so corresponds to the neutral pair (np) ($\text{HCOOH}\cdots\text{NHCH}_2$). The ionic pair (ip) ($\text{HCOO}^-\cdots\text{H}^+\text{NHCH}_2$) corresponds to the right-hand well. (An additional minimum appears in the syn potentials for longer values of $r(\text{OH})$). This minimum is equivalent to the first np structure. After the first proton has transferred across to the N atom, forming the ion pair, the other N—H proton can shift back to the other O atom of HCOO^- , reforming the original $\text{HCOOH}\cdots\text{NHCH}_2$ complex. This possibility is eliminated when the $\theta(\text{CO}\cdots\text{N})$ angle is larger than 120° .) Note that the ion pair is less stable than the neutral pair by some 15–30 kcal/mol, not surprising because the proton affinity of HCOO^- is much higher than that of CH_2NH . The energy barriers for transfer from the left to the right wells are in the range of 30–40 kcal/mol for $R = 3.0$ Å, less than 20 kcal/mol for $R = 2.75$ Å.

As the proton migrates across the H-bond from one species to the next, there is a good deal of angular rearrangement. For example, the $\theta(\text{C—O}\cdots\text{N})$ angle α varies from 100° when $r = 0.9$ Å to 175° when $r = 1.25$ Å to 120° when $r = 1.9$ Å for the syn structure with $R = 2.75$ Å. (The corresponding values of the $\theta(\text{O}\cdots\text{H}\cdots\text{N})$ angle are 157° , 173° , and 155° .) Within the confines of a protein molecule, such reorientation may not be permit-

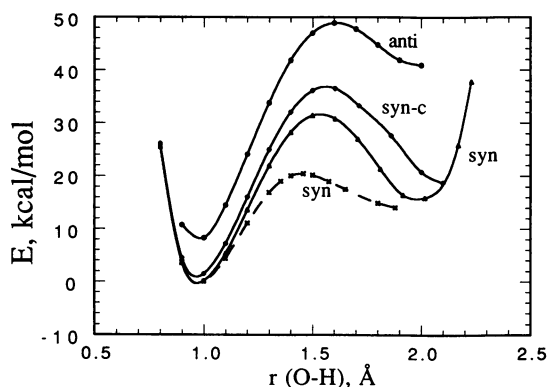


FIGURE 2 Proton transfer potentials computed for various configurations of $\text{HCOO}^-\cdots\text{H}^+\cdots\text{NHCH}_2$. $R(\text{O}\cdots\text{N})$ is equal to 3.0 Å for solid curves, 2.75 Å for broken curve. Energies are relative to that of the neutral pair of the syn conformation.

ted. Moreover, the structural restraints imposed upon the H-bond by the protein may not allow the angle to approach its optimal values (40). We have hence carried out parallel computations for the situation where the above angle is held fixed at one of several values. Specifically, proton transfer potentials were calculated for $\alpha = 90^\circ$, 120° , 150° , and 180° .

The resulting potentials are illustrated for the syn structures, with $\alpha = 120^\circ$, by the curves in Fig. 3 labeled with a 0.0 (indicating the value of g which signifies no external influence here). The left well is considerably lower in energy than the right (ip) well, regardless of angle or intermolecular distance. Results for the anti-geometries are quite similar in that regard. One may conclude that in the absence of external effects, it would be extremely difficult for a Schiff base to hold onto a proton in the presence of a neighboring carboxylate group regardless of the intermolecular angle. One may therefore attribute the likely existence of a protonated Schiff base coupled with a $-\text{COO}^-$ counterion to the mediating influence of the protein.

Upon replacing the $-\text{COO}^-$ ion by $-\text{HO}^-$, one obtains a similar result. Indeed, due to the even greater proton affinity of the latter anion, a righthand well corresponding to the ion pair is completely absent from the potential, even for R as large as 3.0 Å. (A second minimum is present only for the case where $\alpha = 180^\circ$ and is poorly defined even here.)

DIELECTRIC MEDIUM

The nonzero values of g in Fig. 3 refer to potentials computed with the foregoing system placed within a

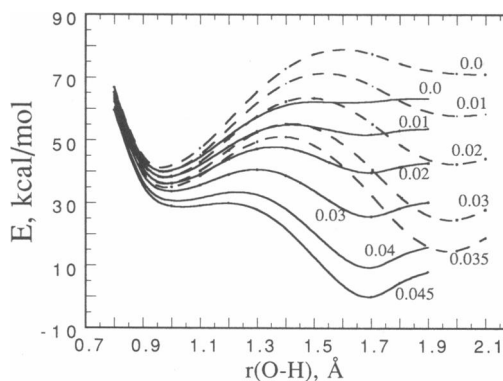


FIGURE 3 Proton transfer potentials computed for syn arrangement with α fixed at 120° . Values of g (numerical labels on each curve) correspond to extent of coupling with polarizable environment (*vide infra*). Solid curves were computed for $R(\text{O}\cdots\text{N}) = 2.75$ Å and broken curves for 3.0 Å. Energies relative to lowest point shown: right well of 2.75 Å curve with $g = 0.045$.

cavity hollowed out of a dielectric continuum, as described above in Methods. Enlargement of the value of g corresponds to increasing dielectric constant of the surrounding medium in the manner prescribed by Eq. 1 above (for each system, g was changed by holding the cavity radius a fixed and varying dielectric constant ϵ . Cavity radii used were set equal to $R(\text{N}\cdots\text{O})$).

In each case, it is clear from Fig. 3 that such a strengthening interaction with the medium leads to a progressive stabilization of the ion pair well on the right. The left well is also lowered in energy but to a much lesser extent. As a specific example, Fig. 4 illustrates the dependence of the energy of both the neutral pair (*solid curves*) and ion pair (*broken curves*) minima as a function of influence of medium for the syn arrangement with $R = 2.75 \text{ \AA}$. Over the course of increasing ϵ from 1 to 50, the neutral pair energies stabilize by perhaps 5–10 kcal/mol. The ion pairs, in contrast, are lowered in energy by as much as 100 kcal/mol.

As an example of the magnitude of the environmental effects, consider the syn geometry where $R = 2.75 \text{ \AA}$ and $\alpha = 120^\circ$. In an in vacuo situation, the neutral pair in which the proton resides on the carboxylate rather than the imine is preferred by some 21 kcal/mol. When g reaches 0.023, however, the two wells are about equal in energy. Stronger interaction results in preferential stabilization of the ion pair, i.e., proton transfer from

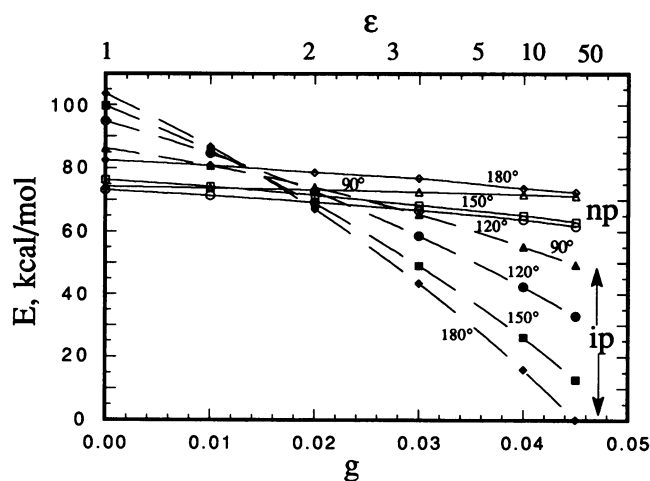


FIGURE 4 SCF energies calculated for neutral pairs (*solid curves*) and ion pairs (*broken curves*) as a function of coupling with the dielectric medium. All curves correspond to the syn arrangement of $\text{HCOO}^-\cdots\text{H}^+\cdots\text{NHCH}_2$ with $R(\text{O}\cdots\text{N}) = 2.75 \text{ \AA}$. Indicated angles refer to $\text{C}-\text{O}\cdots\text{N}$ angle α . Triangle data points represent $\alpha = 90^\circ$; circles, 120° ; squares, 150° ; and diamonds, 180° . Dielectric constants are reported on upper horizontal scale. All energies are on relative scale, with zero taken as the energy of lowest point shown.

carboxylate to imine. This preference grows to nearly 30 kcal/mol when g reaches 0.045.

The shift in proton equilibrium position from one group to the next can be visualized in Fig. 5, where the energy difference between the two wells is presented as a function of coupling with the dielectric medium. For each intermolecular distance R and each angle α considered, it is evident that the environment exerts a strong influence over the relative energies of the neutral and ion pair minima. In vacuo ΔE takes on a value of 17 ± 5 kcal/mol for various angles α for $R = 2.75 \text{ \AA}$. The positive values correspond to preference for the neutral pair versus the ion pair. Increasing g causes a drop in ΔE in all cases although the precise sensitivity varies from one geometry to the next. The syn $\alpha = 180^\circ$ configuration shows the greatest sensitivity, with ΔE decreasing to -70 kcal/mol when g has risen to 0.045. The smaller angle of 120° changes more slowly, diminishing to only -30 kcal/mol over the same range in g ; the 90° configuration undergoes even smaller variation.

This differing sensitivity of ΔE for various values of α produces an important implication. One can take $\Delta(\Delta E) = \Delta E(\alpha = 120^\circ) - \Delta E(\alpha = 180^\circ)$ as a measure of how much influence a 60° change in the intermolecular angle can have upon the shape of the proton transfer potential. Specifically, this quantity reflects the change

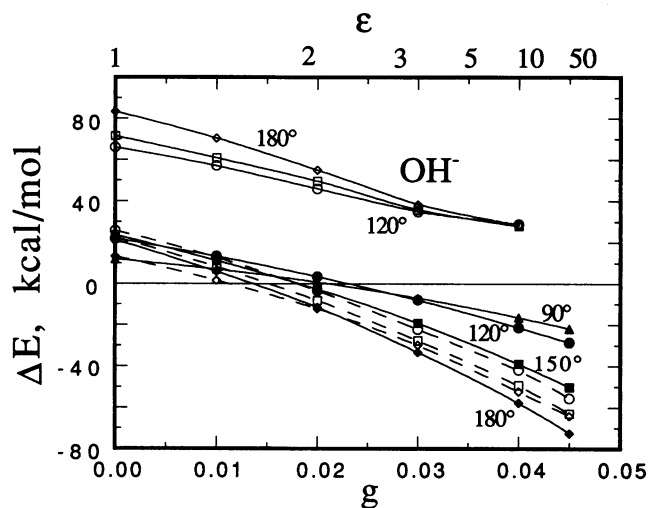


FIGURE 5 Difference in energy, ΔE , between neutral and ion pairs. $\text{HCOO}^-\cdots\text{H}^+\text{NHCH}_2$ system is represented by the lower group of curves: syn conformation (*solid curves*) and anticonformation (*dashed curves*), all for $R = 2.75 \text{ \AA}$. Triangle data points represent $\alpha = 90^\circ$; circles, 120° ; squares, 150° ; and diamonds, 180° . Negative values correspond to greater stability of the ion pair. Upper curves correspond to $\text{HO}^-\cdots\text{H}^+\text{NHCH}_2$ with $R = 3.0 \text{ \AA}$. (Strictly speaking, the potentials for the latter system are of single well type with $g < 0.02$.) Values of ϵ along upper scale apply rigorously only to $\text{HCOO}^-\cdots\text{H}^+\text{NHCH}_2$ system.

in the relative stability of the ion and neutral pair configurations. As illustrated by the solid curves in Fig. 6, the 60° reorientation has essentially no influence upon the competition of the HCOO⁻ and NHCH₂ groups for the proton when $g = 0$; but as g increases, so does $\Delta(\Delta E)$. In fact, when $g = 0.04$ ($\epsilon = 9$), $\Delta(\Delta E)$ has climbed to nearly 40 kcal/mol. At this level of dielectric interaction, then, a 60° reorientation is capable of inducing a change of this amount in the relative proton-attracting power of the HCOO⁻ and NHCH₂ groups. Assuming a temperature of 25°C, this difference corresponds to some 30 pK U, as indicated by the righthand scale of Fig. 6.

One can trace the source of the differing behavior of the three angles back to the energies of the neutral and ion pairs themselves. As Fig. 4 indicates, the change in energy of the neutral pairs as g is increased is essentially identical from one angle to the next; i.e., the four np curves in Fig. 4 are nearly parallel. These neutral pairs are stabilized by the environmental interaction but not to a great extent. The ion pair stabilization is much more extreme. They also behave differently in that the sensitivities of the ip curves to g are greatest for larger angles.

What is it that makes the $\alpha = 180^\circ$ ion pair more sensitive to the external medium? The answer resides in the charge distribution of the complex. The larger angle creates the greatest separation between the noninteracting oxygen of HCOO⁻, which carries a significant fraction of the negative charge, and the CH₂ group of NH₂CH₂⁺. Indeed, the computed dipole moments bear out this notion, with μ increasing from 11.5 D when $\alpha =$

120° to 14.4 D for the 180° angle syn conformation when $R = 2.75 \text{ \AA}$. In contrast, the neutral pairs have a much smaller dipole moment and one much less sensitive to angle. As an illustration, the moments calculated for the 120° and 180° neutral pairs are 4.9 and 4.7 D, respectively.

The situation for the anticonfiguration is similar in that it is still the ion pair that is more sensitive to increasing g . Due to the different location of the carbonyl oxygen of the carboxyl group in the antigeometry, the moment is lessened with larger α , in contrast to the syn trend. As another contrast to the syn case, the dipole moment of the antineutral pair is also sensitive to angle α and in the same sense as the moment of the ion pair. Its energy consequently exhibits a progressively larger stabilization as a function of g for smaller angles. The latter trend of the neutral pair acts to damp the behavior of the ion pair somewhat. The net result is that the broken curves depicting the dependence of ΔE upon g in Fig. 5 are nearly parallel to one another, indicating little sensitivity of this property to intermolecular angle α for the antigeometry. As a consequence of this parallel behavior, the $\Delta(\Delta E)$ curve for the antigeometry in Fig. 6 is rather flat. Nonetheless, this quantity hovers around 10 kcal/mol for all values of g , suggesting that a reduction in α from 180° to 120° can shift the relative pKs of the HCOO⁻ and NHCH₂ groups by some 7 U.

The point at which the neutral and ion pairs become equal in energy is of particular significance as it marks the transition from one type of equilibrium structure to the other. Considering first the syn conformations, characterized by the solid curves in Fig. 5, the $\alpha = 180^\circ$ curve crosses the $\Delta E = 0$ line at $g = 0.014$, whereas the lesser sensitivity when $\alpha = 120^\circ$ causes the transition to be delayed until $g = 0.023$. The dependence of the transition point upon the angle is exhibited in Fig. 7. The upper right portion of the figure corresponds to greater stability of the ion pair while the neutral pair lies to the left of the lines. In each case, one may determine from the figure how a change in α can reverse the relative stabilities of the two complex types.

Taking the anticonformation with $g = 0.015$ as an example, it is clear that increasing this angle from less than 150° to a value greater than this threshold causes the ion pair to be preferred over the neutral pair. That is, when the nitrogen atom of the imine is moved across the line making an angle of 150° with C=O axis, the proton is pulled off of the carboxylate group onto the imine. When g is 0.011 or less, such a shift will not occur because the ion pair is not preferred at any angle. Conversely, it is only the ion pair that exists for $g > 0.018$. It is therefore only in the $0.011 < g < 0.018$ range that the proton position is susceptible to angular changes. The results for the syn conformation are quite compara-

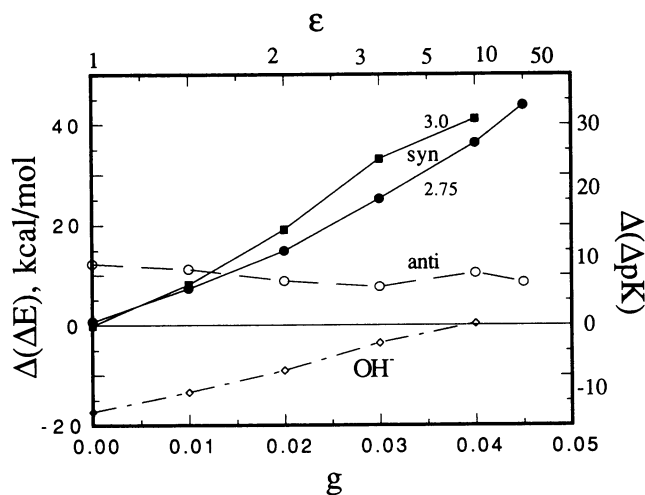


FIGURE 6 Change in ΔE resulting from decreasing angle α from 180° to 120°. Distance R (in \AA) is indicated on the two syn curves; R is equal to 2.75 \AA for the anticonformation of HCOO⁻...⁺HNHCH₂ and 3.0 \AA for HO⁻...⁺HNHCH₂. pK scale on the right side is based on 25°C, also assuming equivalence between energy E and free energy G .

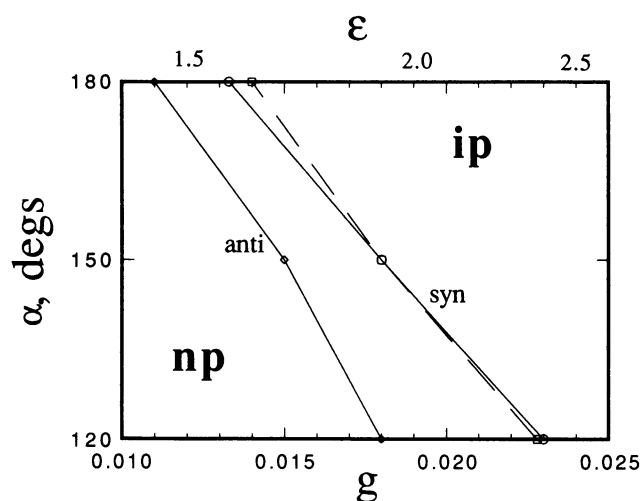


FIGURE 7 Value of α for which neutral and ion pairs are equal in energy as a function of coupling with dielectric medium g . Solid curves refer to $R = 2.75 \text{ \AA}$ and broken curve to 3.0 \AA . Dielectric constants on the upper scale refer to $R = 2.75 \text{ \AA}$. np and ip indicate regions of greater stability of the neutral and ion pairs, respectively.

ble except that the proton-shifting region occurs for g in the range between 0.013 and 0.023. As indicated by the dashed line in Fig. 7, increasing $R(\text{O}\cdots\text{N})$ from 2.75 to 3.0 \AA changes the above trends very little.

The behavior of ΔE for the $\text{HO}^- \cdots \text{H}^+ \cdots \text{NHCH}_2$ complex is illustrated by the upper group of curves in Fig. 5. Note that here again, increasing dielectric makes this quantity less positive. The principal difference is that due to the much higher proton affinity of OH^- as compared with NHCH_2 , even large dielectric coupling is incapable of producing a negative ΔE ; that is, of yielding a more stable ion pair. As in the above case of $\text{HCOO}^- \cdots \text{H}^+ \cdots \text{NHCH}_2$, ΔE is more sensitive to g for larger values of α . This behavior can once again be traced to the greater dipole moments of the ion pair configuration of the large- α geometries. The effect upon proton-attracting power of OH^- versus NHCH_2 is represented by the OH^- curve in Fig. 6 which shows that the 60° reorientation can change the relative pKs by nearly 20 U when $g = 0$ but rapidly diminishes to 0 as g rises to 0.04.

Another important characteristic of the proton transfer potentials is the barrier to proton transfer. The barrier, E^\ddagger , is computed as the difference in energy between the maximum in the potential and the left minimum, corresponding to the neutral pair. This barrier is presented as a function of g for a variety of geometric arrangements in Fig. 8. Not surprisingly, as g increases with its concomitant preferential stabilization of the right side of the potential, the barrier to transfer

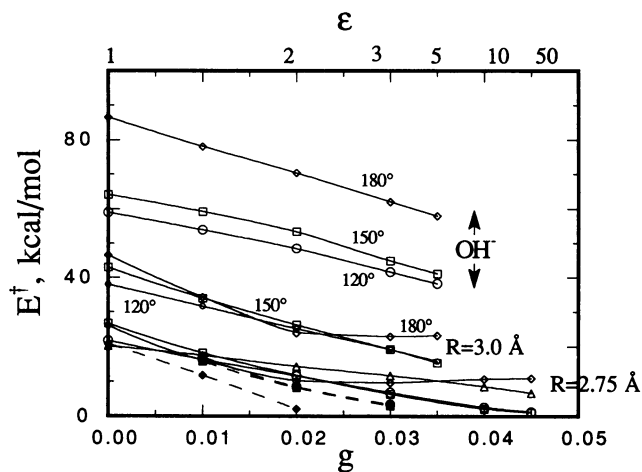


FIGURE 8 Energy barrier to proton transfer from oxygen to nitrogen. Lower groupings of curves refer to E^\ddagger in $\text{HCOO}^- \cdots \text{H}^+ \cdots \text{NHCH}_2$. Solid curves correspond to syn conformation and broken to anticonformation. Triangle data points represent $\alpha = 90^\circ$; circles, 120° ; squares, 150° ; and diamonds, 180° . Upper curves refer to $\text{HOH} \cdots \text{NHCH}_2$, with $R = 3.0 \text{ \AA}$. Values of ϵ along upper scale apply rigorously only to $\text{HCOO}^- \cdots \text{H}^+ \cdots \text{NHCH}_2$ system for which $R = 2.75 \text{ \AA}$.

from neutral to ion pair diminishes. It is interesting that most of the curves in Fig. 8 exhibit a nearly linear dependence of barrier upon g . The principal exception is the syn geometry of $\text{HCOO}^- \cdots \text{H}^+ \cdots \text{NHCH}_2$ when α is equal to 180° , wherein the barriers tend to level off once g has surpassed 0.02 or so. The barriers in the OH^- analogue are presented as the upper group of curves in Fig. 8. These barriers are substantially higher than the equivalent barriers in $\text{HCOO}^- \cdots \text{H}^+ \cdots \text{NHCH}_2$ where R also equals 3.0 \AA . This distinction is easily reconciled on the basis of the much more positive values of ΔE which skew the potentials according to the Hammond postulate (41).

DISCUSSION

It is important to discuss the meaning of these results in the context of a proton transfer that might take place within the confines of a protein. In particular, the Schiff base of bacteriorhodopsin is known to be involved in a proton transfer as part of the proton pumping activity of this protein (5–7). Although the precise nature of the counterion to the protonated Schiff base is not known with certainty, the carboxylate group of an Asp residue appears a likely candidate (6, 24–29). Previous work of a computational nature has suggested that a change in relative orientation between a pair of H-bonding groups such as a Schiff base and carboxyl group can result in a

transfer of a proton from one to the other (16, 18–21, 42). However, these calculations were restricted to an in vacuo environment, not representative of the situation within a protein. The data reported here provide some information as to how the dielectric properties of the protein might affect this transfer.

For example, Fig. 7 suggests that when $g < 0.011$, which corresponds to ϵ of 1.5 or so, the neutral pair is more stable than the ion pair. That is, no matter what interresidue angle is adopted by the H-bonding pair, the proton will prefer association with the carboxylate group. For very large dielectric coupling, on the other hand, it is the protonated Schiff base–carboxylate ion pair that is dominant at any angle. It is in the intermediate region where there is a more subtle interplay between intermolecular angle and level of coupling with the dielectric. It is here where the preference of one configuration or the other is not overwhelmingly decided by the interaction with the medium (or lack thereof). Taking $g = 0.02$ as an example, it is clear from Fig. 7 that decrease of the C=O \cdots N angle α from 150° or so to the 120° range can induce a transfer of the proton from the protonated Schiff base across to the carboxylate in the syn conformation.

Just as the transition from ion to neutral pair can be accomplished by changing the intermolecular angle, Fig. 7 indicates the same sort of transition can accompany an alteration of the interaction of the system with the dielectric medium. Taking the syn conformation with $\alpha = 150^\circ$ as an example again, the system exists preferentially as the ion pair when g is greater than ~ 0.018 . Alterations in the protein environment surrounding the pair that effectively diminishes this interaction would lower g below this threshold and favor the neutral pair instead. Such a change might result from certain geometric adjustments which reorient surrounding polarizable groups or restrict the motion of various groups.

Another important point arising from these calculations is that even a high degree of coupling with a dielectric continuum cannot force the transfer of a proton if the difference in proton affinity between the two species is too large. Specifically, NHCH₂ cannot pull a proton off of a neutral water to form the HO⁻ \cdots H⁺NHCH₂ complex, despite large g and/or changing the intermolecular angle. This finding argues against a water molecule or hydroxyl-containing residue acting as proton-donating counterion in bacteriorhodopsin.

A primary objective of this work has been to compare the pK shift that one can expect as a result of changing the intermolecular orientation within a dielectric medium, as opposed to calculated results in vacuo. Fig. 6 illustrates that reducing the angle α from 180° to 120° can have a dramatic effect indeed. In fact, the change in relative pK can be greater within a dielectric medium

than in vacuo. As an example, shifts of up to 30 pK U are possible for the syn geometry of HCOO⁻ \cdots H⁺ \cdots NHCH₂ with dielectric constants of only 10 or so whereas the pK shift vanishes as ϵ goes to 1.

Of course, pK shifts are only useful concepts if they result in the transfer of the proton across the H-bond. Fig. 7 indicates that such a transfer may occur in the range $0.013 < g < 0.023$ for the syn conformation of HCOO⁻ \cdots H⁺ \cdots NHCH₂. The $\Delta(\Delta pK)$ values for this geometry lie in the range of ~ 5 –12 U according to Fig. 6. Similarly, a change in relative pK of 6–8 is associated with the 60° reorientation within the anticonformation for its range of $0.011 < g < 0.018$.

Coupling of the system with the dielectric properties of the polarizable medium adds another dimension to the proton transfer process. As highlighted in Fig. 8, the barrier to transfer from the oxygen atom to the Schiff base nitrogen drops as g is increased, facilitating formation of the ion pair. At the same time, the barrier for transfer in the reverse direction increases, making it more difficult to destroy the ion pair configuration. So from a kinetic point of view, as well as a thermodynamic perspective discussed above in terms of ΔE , the protonated Schiff base ion pair configuration is favored by progressively more polarizable environment. It should be emphasized that, apart from the changes in barrier height that normally accompany a shifting in energy of the two wells in a Hammond sense, the coupling with the external dielectric appears to have little additional influence upon the barriers.

The reader is cautioned against treating the data presented here in too quantitative a manner. First of all, the HCOO⁻ \cdots H⁺ \cdots NHCH₂ complex represents only a model representation of the aspartate–Schiff base pair in bacteriorhodopsin. Although it does nicely reproduce the relative proton affinities of the two pertinent molecules, and appears to mimic much higher level calculations of proton transfers (8, 43), the 4-31G basis is not without certain weaknesses. Moreover, the SCRF treatment applied to model the interaction of the system with a polarizable continuum does not accurately reproduce all the static and dynamic features of the interaction with a protein molecule. In particular, it ignores some of the aspects of specific short range interactions, e.g., hydrogen bonds. It is suggested that the data be considered rather only in a qualitative sense in order to assess the potential of both angular features of the H-bond and coupling with the protein dielectric for affecting the proton equilibrium position in such systems. For example, the dielectric constants included along the top scale of several of the figures should not be taken literally. It is entirely possible that use of a different basis set, different cavity radius, or modification of the SCRF formalism would affect the data. However, this change would

likely be an overall shift of the entire body of data to higher values of dielectric constant, leaving intact the general trends discussed above.

Correlation is probably not important for our purposes here, as shown by Thole and van Duijnen (44), where dispersion was seen to have little influence upon the relative stability of the neutral and ion pairs, and also plays little role in changing the transfer barrier. Cybulski and Scheiner likewise found that the relative energies of the two wells in a proton transfer potential are often insensitive to correlation (42, 45).

Despite the above limitations, our faith in the theoretical procedure is fortified by an experimental crystal study which confirms our finding that the nature of the surroundings can alter the protonation states of such groups. Specifically, Czugler et al. (46) noted that a proton shifts from a carboxylate group to a nitrogenic imidazole base as the crystal becomes hydrated.

In theoretical studies of related systems, *ab initio* calculations corroborate our own gas-phase result that the neutral pair represents the more stable minimum in the proton transfer potential of an imine-carboxyl complex (47) or guanidinium-carboxylate (48). The ion pair was generally preferred in systems mixing a carboxylate with N bases of various types (49). Jain et al. (50) examined the pair of formic acid plus an imine and found that immersion in a dielectric continuum with an aqueous dielectric constant is capable of making the ion pair competitive in stability with the neutral pair. The SCRF approach taken here to model the surroundings has a long and credible track record which indicates this method can produce results of surprising accuracy (36–39). For the system composed of allylmethylimine and formic acid, the *in vacuo* results suggest the greater stability of the neutral pair, but this preference is reversed when coupling with a dielectric continuum is included (51). Parra-Mouchet et al. (52) found that a solvent dielectric constant in excess of five or so is capable of stabilizing the ion pair over the neutral pair and that this transition point is relatively insensitive to intermolecular distance. Although various combinations of hydrogen halide with amines prefer the neutral pair in the gas phase, the SCRF treatment of solvation leads to ion pairs when the coupling is strong enough (53). The effects of solvation were treated in a discrete fashion by Borstnik et al. (54) who surrounded the ethanolamine-formic acid pair by 207 water molecules and thereby confirmed the ability of solvation to alter the relative stabilities of the neutral and ion pairs.

The ability of an external medium to shift the equilibrium from neutral pair to ion pair has been convincingly demonstrated by spectroscopic means by Zundel's group. For acetic acid-retinal in particular, these measurements indicated the presence of a double minimum

potential in CCl_4 solvent, with the ion pair more stable, i.e., lower enthalpy, by some 2 kcal/mol (55). However, a more favorable entropy leads to observance of the neutral pair. In connection with bacteriorhodopsin itself, Hildebrandt and Stockburger have suggested (56) that the neutral pair would indeed be more stable than the ion pair were it not for the presence of a few key water molecules.

CONCLUSIONS

The equilibrium position of a proton in a system such as $\text{HCOO}^- \cdots \text{H}^+ \cdots \text{NHCH}_2$ depends upon at least two factors. Coupling with the dielectric properties of the surrounding protein favors the charge separation of the ion pair $\text{HCOO}^- \cdots \text{H}^+ \cdots \text{NHCH}_2$, i.e., protonated Schiff base. This proton can be pulled off either by a reduction in the degree of coupling or by a change in the $\text{C}=\text{O} \cdots \text{N}$ intermolecular angle, characterized by α above. The calculations indicate very large relative pK shifts of up to 40 U may be associated with a 60° reorientation. In fact, several groups (57, 58) have previously commented on possible connections between the conformation of the Schiff base and the protonation state of this group and its counterion. But it is only over a certain range of dielectric coupling that the system becomes susceptible to proton transfer via reorientation. Within this range, the maximum pK shifts associated with this reorientation are between 5 and 12. In a more general sense, it must also be realized that even a high degree of coupling or large scale reorientation cannot cause a proton to transfer from A to B if the deprotonation energy of AH^+ is much larger than that of BH^+ .

The results for the syn and anticonformations of the $\text{HCOO}^- \cdots \text{H}^+ \cdots \text{NHCH}_2$ complex are fairly similar to one another in that both show an increasing tendency for ion pair formation at higher ϵ and for larger $\text{C}=\text{O} \cdots \text{N}$ angle. The principal difference is that the anticonformation forms the ion pair more readily in that it requires a smaller value of ϵ to favor the ion over the neutral pair. The relative pK shifts associated with a 60° reorientation within the anticonformation are ~ 7 U for all dielectric constants while $\Delta(\Delta\text{pK})$ rises with increasing ϵ for the syn. It should finally be noted that the dynamics of proton transfer are consistent with the above trends in that as the ion pair becomes preferentially stabilized relative to the neutral pair, the energy barrier for formation of the former from the latter is lowered.

We are grateful to Dr. Robert Brenstein and Mr. C. Frederick Sahlen for carrying out some initial calculations. Professor R. A. Mathies kindly provided a preprint of his work and helpful discussions.

This work was supported financially by the National Institutes of Health (GM-29391).

Received for publication 28 January 1991 and in final form 10 June 1991.

REFERENCES

1. Howell, E. E., J. E. Villafranca, M. S. Warren, S. J. Oatley, and J. Kraut. 1986. Functional role of aspartic acid-27 in dihydrofolate reductase revealed by mutagenesis. *Science (Wash. DC)*. 231: 1123–1128.
2. Silverman, D. N., and S. H. Vincent. 1983. Proton transfer in the catalytic mechanism of carbonic anhydrase. *CRC Crit. Rev. Biochem.* 14:207–255.
3. Cho, Y.-K., and P. F. Cook. 1989. pH dependence of the kinetic parameters for the pyrophosphate-dependent phosphofructokinase reaction supports a proton-shuttle mechanism. *Biochemistry*. 28:4155–4160.
4. Craik, C. S., S. Roczniak, C. Largman, and W. J. Rutter. 1987. The catalytic role of the active site aspartic acid in serine proteases. *Science (Wash. DC)*. 237:909–913.
5. Braiman, M. S., T. Mogi, T. Marti, L. J. Stern, H. G. Khorana, and K. J. Rothschild. 1988. Vibrational spectroscopy of bacteriorhodopsin mutants: light-driven proton transport involves protonation changes of aspartic acid residues 85, 96, and 212. *Biochemistry*. 27:8516–8520.
6. Lin, S. W., and R. A. Mathies. 1989. Orientation of the protonated retinal Schiff base group in bacteriorhodopsin from absorption linear dichroism. *Biophys. J.* 56:653–660.
7. Pollard, H.-J., M. A. Franz, W. Zinth, W. Kaiser, E. Kolling, and D. Oesterhelt. 1986. Early picosecond events in the photocycle of bacteriorhodopsin. *Biophys. J.* 49:651–662.
8. Scheiner, S. 1985. Theoretical studies of proton transfer. *Acc. Chem. Res.* 18:174–180.
9. Scheiner, S. 1988. Relationships between the angular characteristics of a hydrogen bond and the energetics of proton transfer occurring within. *J. Mol. Struct. (Theochem.)*. 177:79–91.
10. Pardo, L., A. P. Mazurek, and R. Osman. 1990. Computational models for proton transfer in biological systems. *Int. J. Quantum Chem.* 37:701–711.
11. Bosch, E., J. M. Lluch, and J. Bertran. 1990. Symmetric intramolecular proton transfers between oxygen atoms in anionic systems. An *ab initio* study. *J. Am. Chem. Soc.* 112:3868–3874.
12. Jones, W. H., P. G. Mezey, and I. G. Csizmadia. 1985. Proton transfer in the ethylene-hydronium ion complex. *J. Mol. Struct. (Theochem.)*. 121:85–92.
13. Cao, H. Z., M. Allavena, O. Tapia, and E. M. Evleth. 1985. Theoretical analysis of proton transfers in symmetric and asymmetric systems. *J. Phys. Chem.* 89:1581–1592.
14. Scheiner, S. 1981. Proton transfers in hydrogen-bonded systems. Cationic oligomers of water. *J. Am. Chem. Soc.* 103:315–320.
15. Scheiner, S. 1982. Comparison of proton transfers in heterodimers and homodimers of NH_3 and OH_2 . *J. Chem. Phys.* 77:4039–4050.
16. Hillenbrand, E. A., and S. Scheiner. 1986. Analysis of principles governing proton-transfer reactions. Carboxyl group. *J. Am. Chem. Soc.* 108:7178–7186.
17. Scheiner, S., and Z. Latajka. 1987. Kinetics of proton transfer in $(\text{H}_3\text{CH}\cdots\text{CH}_2)^+$. *J. Phys. Chem.* 91:724–730.
18. Hillenbrand, E. A., and S. Scheiner. 1985. Analysis of the principles governing proton-transfer reactions. Comparison of the imine and amine groups. *J. Am. Chem. Soc.* 107:7690–7696.
19. Scheiner, S., and E. A. Hillenbrand. 1985. Modification of pK values caused by change in H-bond geometry. *Proc. Natl. Acad. Sci. USA*. 82:2741–2745.
20. Cybulski, S. M., and S. Scheiner. 1989. Factors contributing to distortion energies of bent hydrogen bonds. Implications for proton-transfer potentials. *J. Phys. Chem.* 93:6565–6574.
21. Cybulski, S. M., and S. Scheiner. 1990. Factors contributing to distortion energies of bent hydrogen bonds. 2. Imine, carbonyl, carboxyl, and carboxylate groups. *J. Phys. Chem.* 94:6106–6116.
22. Scheiner, S., P. Redfern, and M. M. Szczesniak. 1985. Effects of external ions on the energetics of proton transfers across hydrogen bonds. *J. Phys. Chem.* 89:262–266.
23. Kurnig, I. J., and S. Scheiner. 1986. Additivity of the effects of external ions and dipoles upon the energetics of proton transfer. *Int. J. Quantum Chem. QBS13*:71–79.
24. Dunach, M., S. Berkowitz, T. Marti, Y.-W. He, S. Subramanian, H. G. Khorana, and K. J. Rothschild. 1990. Ultraviolet-visible transient spectroscopy of bacteriorhodopsin mutants. *J. Biol. Chem.* 265:16978–16984.
25. Holz, M., L. A. Drachev, T. Mogi, H. Otto, A. D. Kaulen, M. P. Heyn, V. P. Skulachev, and H. G. Khorana. 1989. Replacement of aspartic acid-96 by asparagine in bacteriorhodopsin slows both the decay of the M intermediate and the associated proton movement. *Proc. Natl. Acad. Sci. USA*. 86:2167–2171.
26. Eisenstein, L., S.-L. Lin, G. Dollinger, K. Odashima, J. Termini, K. Konno, W.-D. Ding, and K. Nakanishi. 1987. FTIR difference studies on apoproteins. Protonation states of aspartic and glutamic acid residues during the photocycle of bacteriorhodopsin. *J. Am. Chem. Soc.* 109:6860–6862.
27. Gerwert, K., B. Hess, J. Soppa, and D. Oesterhelt. 1989. Role of aspartate-96 in proton translocation by bacteriorhodopsin. *Proc. Natl. Acad. Sci. USA*. 86:4943–4947.
28. Alshuth, A., and M. Stockburger. 1986. Time-resolved resonance Raman studies on the photochemical cycle of bacteriorhodopsin. *Photochem. Photobiol.* 43:55–66.
29. Mathies, R. A., S. W. Lin, J. B. Ames, and W. T. Pollard. 1991. From femtoseconds to biology: mechanism of bacteriorhodopsin's light-driven proton pump. *Annu. Rev. Biophys. Biophys. Chem.* In press.
30. Ditchfield, R., W. J. Hehre, and J. A. Pople. 1971. Self-consistent molecular-orbital methods. IX. An extended Gaussian-type basis for molecular-orbital studies of organic molecules. *J. Chem. Phys.* 54:724–728.
31. Frisch, M. J., J. S. Binkley, H. B. Schlegel, K. Raghavachari, C. F. Melius, J. L. Martin, J. J. P. Stewart, F. W. Bobrowicz, C. M. Rohlfing, L. R. Kahn, D. J. DeFrees, R. Seeger, R. A. Whiteside, D. J. Fox, E. M. Fleuder, and J. A. Pople. 1984. GAUSSIAN 86. Carnegie-Mellon Quantum Chemistry Publishing Unit, Pittsburgh, PA; Frisch, M. J., M. Head-Gordon, H. B. Schlegel, K. Raghavachari, J. S. Binkley, C. Gonzalez, D. J. DeFrees, D. J. Fox, R. A. Whiteside, R. Seeger, C. F. Melius, J. Baker, R. Martin, L. R. Kahn, J. J. P. Stewart, E. M. Fleuder, S. Topiol, and J. A. Pople. 1988. GAUSSIAN 88. Pittsburgh, PA.
32. Peterson, M. R., and R. A. Poirier. 1984. MONSTERGAUSS. Department of Chemistry, University of Toronto, Ontario, M5S 1A1, Canada.

33. Del Bene, J. E. 1984. Geometry, basis set, and correlation energy dependence of computed protonation energies of imino bases. *J. Comput. Chem.* 5:381–386.
34. Ewig, C. S., and J. R. Van Wazer. 1986. *Ab initio* studies of molecular structures and energetics. 1. Base-catalyzed hydrolysis of simple formates and structurally related reactions. *J. Am. Chem. Soc.* 108:4774–4783.
35. Bartmess, J. E., and R. T. McIver, Jr. 1979. The gas-phase acidity scale. In *Gas Phase Ion Chemistry*. M. T. Bowers, editor. Academic Press: New York. Vol. 2:87–121.
36. Sanhueza, J. E., and O. Tapia. 1982. The quantum chemical calculation of environmental effects: a comparative study of charge separation in water dimers. *J. Mol. Struct. (Theochem.)*. 89:131–146.
37. Tapia, O., F. M. L. G. Stamato, and Y. G. Smeyers. 1985. Modeling active site response towards changes in the protein-core of serine proteases. A CNDO/2-INDO SCRF study of subtilisin and thiosubtilisin. *J. Mol. Struct. (Theochem.)*. 123:67–84.
38. Tapia, O., F. Sussman, and E. Poulain. 1978. Environmental effects on H-bond potentials: a SCRF MO CNDO/2 study of some model systems. *J. Theor. Biol.* 71:49–72.
39. Tapia, O., E. Poulain, and F. Sussman. 1975. Hydrogen bond environmental effects on proton potential curves. An SCRF MO CNDO/2 calculation of a water dimer. *Chem. Phys. Lett.* 33:65–70.
40. Baker, E. N., and R. E. Hubbard. 1984. Hydrogen bonding in globular proteins. *Prog. Biophys. Mol. Biol.* 44:97–179.
41. Hammond, G. S. 1955. A correlation of reaction rates. *J. Am. Chem. Soc.* 77:334–338.
42. Cybulski, S. M., and S. Scheiner. 1989. Hydrogen bonding and proton transfers involving the carboxylate group. *J. Am. Chem. Soc.* 111:23–31.
43. Scheiner, S., and L. B. Harding. 1983. Molecular orbital study of proton transfer in $(\text{H}_3\text{NHOH}_2)^+$. *J. Phys. Chem.* 87:1145–1153.
44. Thole, B. T., and P. T. van Duijnen. 1983. Reaction field effects on proton transfer in the active site of actinidin. *Biophys. Chem.* 18:53–59.
45. Cybulski, S. M., and S. Scheiner. 1987. Hydrogen bonding and proton transfers involving triply bonded atoms. $\text{HC}\equiv\text{CH}$ and $\text{HC}\equiv\text{N}$. *J. Am. Chem. Soc.* 109:4199–4206.
46. Czugler, M., J. G. Angyan, and G. Naray-Szabo. 1986. Noncovalent structural models for the Asp–His dyad in the active site of serine proteases and for solid-state switching of protonation states: crystal structure of the associates of 1,1'-binaphthyl-2,2'-dicarboxylic acid with imidazole in dihydrated and in anhydrous forms. *J. Am. Chem. Soc.* 108:1275–1281.
47. Fugler, L., C. S. Russell, and A. M. Sapse. *Ab initio* calculations on imine–carboxyl complexes. *J. Phys. Chem.* 91:37–41.
48. Sapse, A. M., and C. S. Russell. 1986. Theoretical studies of the binding of methylamine and guanidine to carboxylate. *J. Mol. Struct. (Theochem.)*. 137:43–53.
49. Hodoscek, M., D. Hadzi, and T. Solmajer. 1989. *Ab initio* calculations of hydrogen bonding between guanidine isosters and carboxylate. *J. Mol. Struct. (Theochem.)*. 183:371–379.
50. Jain, D. C., A. M. Sapse, and D. Cowburn. 1988. Solvent effect on some imine–carboxyl complexes. *J. Phys. Chem.* 92:6847–6849.
51. Hadzi, D., J. Koller, and M. Hodoscek. 1988. *Ab initio* calculations of proton potential functions of some rhodopsin modeling systems. *J. Mol. Struct. (Theochem.)*. 168:279–286.
52. Parra-Mouchet, J., R. R. Contreras, and A. Aizman. 1988. Self-consistent reaction field calculations on the proton transfer in ammonia–formic acid systems as a model for hydrogen bonding in solution. *Int. J. Quantum Chem.* 33:41–52.
53. Kurnig, I. J., and S. Scheiner. 1987. *Ab initio* investigation of the structure of hydrogen halide–amine complexes in the gas phase and in a polarizable medium. *Int. J. Quantum Chem.* QBS14:47–56.
54. Borstnik, B., D. Janezic, and D. Hadzi. 1986. Monte Carlo study of ethanolamine–formic acid hydration effect of proton transfer. *J. Mol. Struct.* 138:341–352.
55. Merz, H., and G. Zundel. 1986. Thermodynamics of proton transfer in carboxylic acid–retinal Schiff base hydrogen bonds with large proton polarizability. *Biochem. Biophys. Res. Commun.* 138:819–825.
56. Hildebrandt, P., and M. Stockburger. 1984. Role of water in bacteriorhodopsin's chromophore: resonance Raman study. *Biochemistry*. 23:5539–5548.
57. Sharkov, A. V., A. V. Pakulev, S. V. Chekalin, and Y. A. Matveetz. 1985. Primary events in bacteriorhodopsin probed by subpicosecond spectroscopy. *Biochim. Biophys. Acta.* 808:94–102.
58. Sheves, M., A. Albeck, N. Friedman, and M. Ottolenghi. 1986. Controlling the pKa of the bacteriorhodopsin Schiff base by use of artificial retinal analogues. *Proc. Natl. Acad. Sci. USA.* 83:3262–3266.